

Memory effect in uniformly heated granular gases

E. Trizac¹ and A. Prados^{1,2}

¹ *Université Paris-Sud, Laboratoire de Physique Théorique et Modèles Statistiques,
UMR CNRS 8626, 91405 Orsay, France, EU and*

² *Física Teórica, Universidad de Sevilla, Apartado de Correos 1065, E-41080 Sevilla, Spain, EU*
(Dated: March 2, 2022)

We evidence a Kovacs-like memory effect in a uniformly driven granular gas. A system of inelastic hard particles, in the low density limit, can reach a non-equilibrium steady state when properly forced. By following a certain protocol for the drive time dependence, we prepare the gas in a state where the granular temperature coincides with its long time value. The temperature subsequently does not remain constant, but exhibits a non-monotonic evolution with either a maximum or a minimum, depending on the dissipation, and on the protocol. We present a theoretical analysis of this memory effect, at Boltzmann-Fokker-Planck equation level, and show that when dissipation exceeds a threshold, the response can be coined anomalous. We find an excellent agreement between the analytical predictions and direct Monte Carlo simulations.

PACS numbers: 45.70.-n, 05.20.Dd, 51.10.+y, 02.70.-c

I. INTRODUCTION

A granular material is a system comprising a large number of particles of macroscopic size, so that the collisions between them are inelastic and mechanical energy is not conserved. As consequence, the usual thermodynamical framework cannot be directly applied to these systems. Typically, the energy needed to move a grain by one diameter is many orders of magnitude larger than the thermal energy of the grain at room temperature, which can be considered irrelevant for all practical purposes. On the other hand, the concept of *granular temperature* is often used in the literature; it is nothing but a measure of the velocity fluctuations in the system, without being connected to any notion of thermal equilibrium [1, 2].

We focus here on a low density granular system, which is usually called a granular gas [3, 4]. If no energy is input into the system, it freely cools (in the sense that its granular temperature monotonically decreases) and may end up in the homogeneous cooling state [5–7], provided instabilities are circumvented by the choice of a small enough system. The time dependence of the system can then solely be encoded in the granular temperature, which in turn verifies Haff’s law [8]. On the other hand, if there is some mechanism that feeds energy into the system, it eventually reaches a non-equilibrium steady state in which energy input by the *thermostat* balances in average the energy loss due to collisions. To the best of our knowledge, and although this kind of thermostatted or heated granular fluids have been extensively investigated [7, 9–18], no attention has been paid to the possible existence of memory effects. On the other hand, in other experiments with granular matter like compaction processes, memory effects have been analyzed both experimentally and theoretically [19–24]. They have shown that, in general, the evolution of a compacting granular system depends not only on the instantaneous value of its packing fraction but also on its previous history.

A classic experiment in this context is the one per-

formed by Kovacs fifty years ago [25, 26]. A sample of polyvinyl acetate was equilibrated by putting it in a thermal bath at a high temperature T_0 , and then was rapidly quenched to a low temperature T_1 . At this low temperature, it relaxed for a given *waiting time* t_w . At time $t = t_w$, the bath temperature was suddenly raised to an intermediate temperature T , $T_0 > T > T_1$, such that the instantaneous value of the polymer volume at $t = t_w$ was equal to its equilibrium value at T . The behavior of the system for $t > t_w$ was quite complex: The volume did not remain constant, but increased at first, passing through a maximum, and relaxed to equilibrium only for longer times. As the pressure P was kept fixed along all the process, the observed behavior means that the knowledge of the state variables (P, V, T) does not suffice to completely characterize the state of the system. The system evolution from an initial state with given values of (P, V, T) depends on the previous thermal history. This behavior is sometimes referred to in the literature as the Kovacs hump, and it has been extensively studied in glassy and other complex systems [21, 27–34]. In many of these works, the physical quantity displaying the Kovacs hump is the energy instead of the volume. In connection with the work presented here, it should be emphasized that the granular temperature is essentially the internal energy of the granular gas. We refer to the driving program in which $T_1 < T < T_0$ as the “cooling” protocol. Conversely, a “heating” protocol in which the temperature jumps are reversed and $T_1 > T > T_0$ has been recently considered [33]. Within this scheme, the relevant physical quantity, typically the volume or the energy, displays a minimum instead of a maximum.

First, it is important to stress that a relevant question is the number and type of variables characterizing the macroscopic state of granular gases. In the homogeneous cooling state [5–7], and also in the Gaussian thermostatted case [11, 35, 36], the granular temperature suffices. For other energy injection mechanisms, like the stochastic thermostat, there is some evidence that additional vari-

ables must be taken into account: This uniformly driven granular gas evolves to a hydrodynamic solution (β -state) of the kinetic equation [16, 17], over which the granular temperature is a monotonic function of time. In addition, the granular temperature and the driving intensity characterize the β -state completely, a behavior that may lead to the conclusion that no Kovacs hump should be expected. We show here that this speculative conclusion is flawed: the Kovacs effect is indeed present in driven granular gasses and, moreover, it changes sign with inelasticity.

In light of the discussion above, it seems worthwhile to investigate the possible existence of memory effects in driven granular gases. The steady value of the granular temperature is a certain function of the driving intensity, which is the externally controlled parameter in this case. Thus, the granular temperature plays the role of the volume in the Kovacs experiment, while the intensity of the driving is the analogue of the bath temperature: we may start from the stationary state corresponding to a high value of the driving, and let the system relax to a new steady state by rapidly quenching the driving to a low value. This relaxation is subsequently interrupted after a waiting time t_w , and the driving is readjusted to an intermediate value, whose corresponding steady granular temperature equals its instantaneous value at the waiting time. The existence or non-existence of a Kovacs hump in this program undoubtedly answers whether the granular temperature, together with the driving intensity, thoroughly characterizes or not the state of the heated granular system.

In this paper, we investigate the existence of such a hump in the granular temperature when the above sketched stepwise driving program, à la Kovacs, is implemented in an homogeneously driven granular gas. We do this analysis both in the usual “cooling” protocol (by decreasing the driving from its initial value) and for the “heating” protocol (by increasing the driving from its initial value). In both cases, we show that the granular temperature indeed displays this Kovacs hump, thus proving that the granular temperature does not uniquely characterize the state of the granular system. This is in agreement with recent investigations in the so-called universal reference state [16], which plays the main role in the derivation of linear hydrodynamics for driven granular gases [17]. However, it will appear that an additional quantity should be kept in the dynamical description, measuring non-Gaussianities. Interestingly, there is a value of the restitution coefficient for which the sign of the hump reverses. For the cooling (resp. heating) protocol, while the granular temperature has a maximum (resp. minimum) for high enough restitution coefficient (small inelasticities), it shows a minimum (resp. maximum) when the restitution coefficient is smaller than a critical one (high inelasticities). The theoretical results, obtained from the Boltzmann-Fokker-Planck equation, by (i) considering the first Sonine approximation and (ii) neglecting nonlinear terms in the excess kurtosis,

are compared to direct Monte Carlo simulations thereof, and an excellent agreement is found. It is also shown that the expression of the Kovacs hump so obtained tends to the universal reference state [16] for very long times.

The plan of the paper is as follows. In Sec. II, we introduce our model and summarize some of the previous results that are relevant for the work presented here. In particular, we write the evolution equations for both the granular temperature and the excess kurtosis of the velocity distribution function. We put forward a Kovacs-like program for the driving in Sec. III, and obtain approximate analytical expressions for the time evolution of both the granular temperature and the excess kurtosis. These analytical expressions are compared to direct Monte Carlo simulation results. We present a physical discussion of the sign and magnitude of the memory effect in Sec. IV. We also discuss the long time limit and the tendency to the universal reference state in Sec. V. Some final remarks, relevant to put our work in a proper context, are presented in Section VI. Preliminary accounts on parts of this work were published in [37].

II. UNIFORMLY HEATED GRANULAR GAS

We consider a system of N inelastic smooth hard particles of mass m and diameter σ . The collisions between them are inelastic and characterized by the coefficient of normal restitution α , which we assume does not depend on the relative velocity. In a binary collision of particles i and j , the relation between the pre-collisional velocities $(\mathbf{v}_i, \mathbf{v}_j)$ and the post-collisional velocities $(\mathbf{v}'_i, \mathbf{v}'_j)$ is

$$\mathbf{v}'_i = \mathbf{v}_i - \frac{1+\alpha}{2} (\hat{\boldsymbol{\sigma}} \cdot \mathbf{v}_{ij}) \boldsymbol{\sigma}, \quad \mathbf{v}'_j = \mathbf{v}_j + \frac{1+\alpha}{2} (\hat{\boldsymbol{\sigma}} \cdot \mathbf{v}_{ij}) \boldsymbol{\sigma}, \quad (1)$$

where $\mathbf{v}_{ij} \equiv \mathbf{v}_i - \mathbf{v}_j$ is the relative velocity and $\hat{\boldsymbol{\sigma}}$ is the unit vector pointing from the center of particle j to the center of particle i at the collision. Moreover, independent white noise forces act over each grain, so that the following Boltzmann-Fokker-Planck equation holds for a homogeneous system [7, 10],

$$\begin{aligned} \frac{\partial}{\partial t} f(\mathbf{v}_1, t) = & \sigma^{d-1} \int d\mathbf{v}_2 \bar{T}_0(\mathbf{v}_1, \mathbf{v}_2) f(\mathbf{v}_1, t) f(\mathbf{v}_2, t) \\ & + \frac{\xi^2}{2} \frac{\partial^2}{\partial \mathbf{v}_1^2} f(\mathbf{v}_1, t), \end{aligned} \quad (2)$$

where d is the dimension of space, ξ is a measure of the noise intensity, and \bar{T}_0 is the binary collision operator defined by

$$\bar{T}_0(\mathbf{v}_1, \mathbf{v}_2) = \int d\hat{\boldsymbol{\sigma}} \Theta(\mathbf{v}_{12} \cdot \hat{\boldsymbol{\sigma}}) (\mathbf{v}_{12} \cdot \hat{\boldsymbol{\sigma}}) (\alpha^{-2} b_{\sigma}^{-1} - 1). \quad (3)$$

In the equation above, the operator b_{σ}^{-1} replaces the velocities \mathbf{v}_1 and \mathbf{v}_2 by the precollisional ones, which would be obtained by inverting (1). We assume here that the system remains spatially homogeneous, which is backed

up by molecular dynamics simulations [10]: the velocity probability distribution f is thus a sole function of velocity and time.

The granular temperature $T(t)$ is defined as usual,

$$n \left\langle \frac{1}{2} m v^2(t) \right\rangle \equiv \int d\mathbf{v} \frac{1}{2} m v^2 f(\mathbf{v}, t) = \frac{d}{2} n T(t), \quad (4)$$

where n is the density of the system. Moreover, we also introduce the *excess kurtosis* or second Sonine coefficient a_2 of the velocity distribution,

$$a_2 = \frac{d}{d+2} \frac{\langle v^4 \rangle}{\langle v^2 \rangle^2} - 1. \quad (5)$$

The excess kurtosis measures the departure from a Gaussian distribution, for which a_2 vanishes. It is worth remembering that $\int d\mathbf{v} f(\mathbf{v}, t) = n$, so that

$$\langle v^n \rangle \equiv \frac{1}{n} \int d\mathbf{v} v^n f(\mathbf{v}, t). \quad (6)$$

Starting from the Boltzmann-Fokker-Planck equation (2), one can derive the equation governing the time evolution of the granular temperature

$$\frac{dT}{dt} = m\xi^2 - \zeta_0 T^{3/2} \left(1 + \frac{3}{16} a_2 \right), \quad (7)$$

where

$$\zeta_0 = \frac{2n\sigma^{d-1} (1 - \alpha^2) \pi^{\frac{d-1}{2}}}{\sqrt{m} d \Gamma(d/2)}. \quad (8)$$

Equation (7) is valid in the so-called first Sonine approximation, and terms of $\mathcal{O}(a_2^2)$ are neglected in its derivation [7] together with higher order contributions, that do not seem to be relevant [38]. In other words, the velocity distribution is expanded in the form,

$$f(\mathbf{v}, t) = \frac{e^{-v^2/v_0^2}}{v_0^d \pi^{d/2}} [1 + a_2 S_2(v/v_0)], \quad (9)$$

$$S_2(x) = \frac{1}{2} x^4 - \frac{d+2}{2} x^2 + \frac{d(d+2)}{8} \quad (10)$$

where v_0 is the time dependent typical velocity defined by $T = m v_0^2/2$, and $S_2(x)$ is the second Sonine polynomial. Sonine-related techniques are often useful in kinetic theory [39], to study the non equilibrium behaviour

of dissipative gases [22] or in the context of ballistically controlled irreversible dynamics [40, 41].

In the long time limit, the system approaches a steady state in which the energy input due to the white noise force balances on average the energy loss due to the collisions. Therefore, the granular temperature T and the excess kurtosis a_2 approach their steady values T_s and a_2^s , respectively, which verify

$$m\xi^2 = \zeta_0 T_s^{3/2} \left(1 + \frac{3}{16} a_2^s \right). \quad (11)$$

The evolution equation (7) or its particularization to the steady state (11) are not closed for the granular temperature, because of the terms proportional to the excess kurtosis in them. The steady value of the excess kurtosis can be calculated in the first Sonine approximation [7, 12]

$$a_2^s = \frac{16(1 - \alpha)(1 - 2\alpha^2)}{73 + 56d - 24d\alpha - 105\alpha + 30(1 - \alpha)\alpha^2}. \quad (12)$$

Then, the steady value of the temperature is

$$T_s = m \left[\frac{d\Gamma(d/2)\xi^2}{2\pi^{\frac{d-1}{2}} n \sigma^{d-1} (1 - \alpha^2) (1 + \frac{3}{16} a_2^s)} \right]^{2/3}. \quad (13)$$

Let us turn Eq. (7) into an evolution equation for the dimensionless variable

$$\beta = \sqrt{\frac{T_s}{T}} \quad (14)$$

that measures the separation of the temperature from its steady value. A simple calculation yields

$$\frac{d\beta}{dt} = \frac{\zeta_0}{2} \sqrt{T_s} \left[1 + \frac{3}{16} a_2 - \left(1 + \frac{3}{16} a_2^s \right) \beta^3 \right]. \quad (15)$$

The evolution equation for the excess kurtosis can also be derived from the Boltzmann-Fokker-Planck equation [16]. We again consider the first Sonine approximation and neglect nonlinear terms in the excess kurtosis, to obtain that

$$\beta \frac{da_2}{dt} = 2\zeta_0 \sqrt{T_s} [(1 - \beta^3) a_2 + B(a_2^s - a_2)]. \quad (16)$$

The parameter B has been computed in [16, 42], with the result

$$B = \frac{73 + 8d(7 - 3\alpha) + 15\alpha[2\alpha(1 - \alpha) - 7]}{16(1 - \alpha)(3 + 2d + 2\alpha^2) + a_2^s[85 + d(62 - 30\alpha) + 3\alpha(10\alpha(1 - \alpha) - 39)]}, \quad (17)$$

which is then a given function of the restitution coefficient

and of the dimension of space. It turns out, however, that

it can be obtained from a self-consistent argument [37]. In the limit where the forcing ξ is so small that $\beta \rightarrow 0$, the excess kurtosis should evolve to its homogeneous cooling state value, given by [12]

$$a_2^{\text{HCS}} = \frac{16(1-\alpha)(1-2\alpha^2)}{25+2\alpha(\alpha-1)+24d+\alpha(8d-57)}. \quad (18)$$

This yields a strong constraint on B , which has to be compatible with this requirement. In other words, the right hand side of Eq. (16), when β can be neglected, should admit a_2^{HCS} as a root. Thus,

$$a_2^{\text{HCS}} + B(a_2^s - a_2^{\text{HCS}}) = 0 \quad (19)$$

from which we obtain that

$$B = \frac{a_2^{\text{HCS}}}{a_2^{\text{HCS}} - a_2^s} \quad (20)$$

$$= \frac{73 + 8d(7-3\alpha) + 15\alpha[2\alpha(1-\alpha) - 7]}{16(1-\alpha)(3+2d+2\alpha^2)}. \quad (21)$$

This expression, interestingly, is derived in a more straightforward way than in Ref. [16]. They differ by the term proportional to a_2^s in the denominator of Eq. (17), which reduces to Eq. (21) if this term is omitted. In the following analysis, we will make use of Eq. (21) instead of Eq. (17), since it turns out to be more accurate as compared to simulation results. In addition, this is consistent with the linearization in a_2 in Eq. (16): Therein, B multiplies $a_2 - a_2^s$, so that any terms proportional to the excess kurtosis in B should be neglected.

Equation (16), together with (15), constitute a closed set of two differential equations for the time evolution of the rescaled temperature β and the excess kurtosis a_2 . We can also introduce a rescaled excess kurtosis

$$A_2 = \frac{a_2}{a_2^s}, \quad A_2^s = 1, \quad (22)$$

and rewrite Eqs. (15) and (16) in the following way,

$$\frac{d\beta}{d\tau} = 1 - \beta^3 + \frac{3}{16}a_2^s(A_2 - \beta^3), \quad (23a)$$

$$\beta \frac{dA_2}{d\tau} = 4[(1-\beta^3)A_2 + B(1-A_2)], \quad (23b)$$

where we have introduced a rescaled time

$$\tau = \frac{\zeta_0 \sqrt{T_s}}{2} t. \quad (24)$$

Equations (23) are nonlinear in β but linear in the excess kurtosis, consistently with our approach. Obviously, $\beta = 1$ and $A_2 = 1$ is a stationary solution.

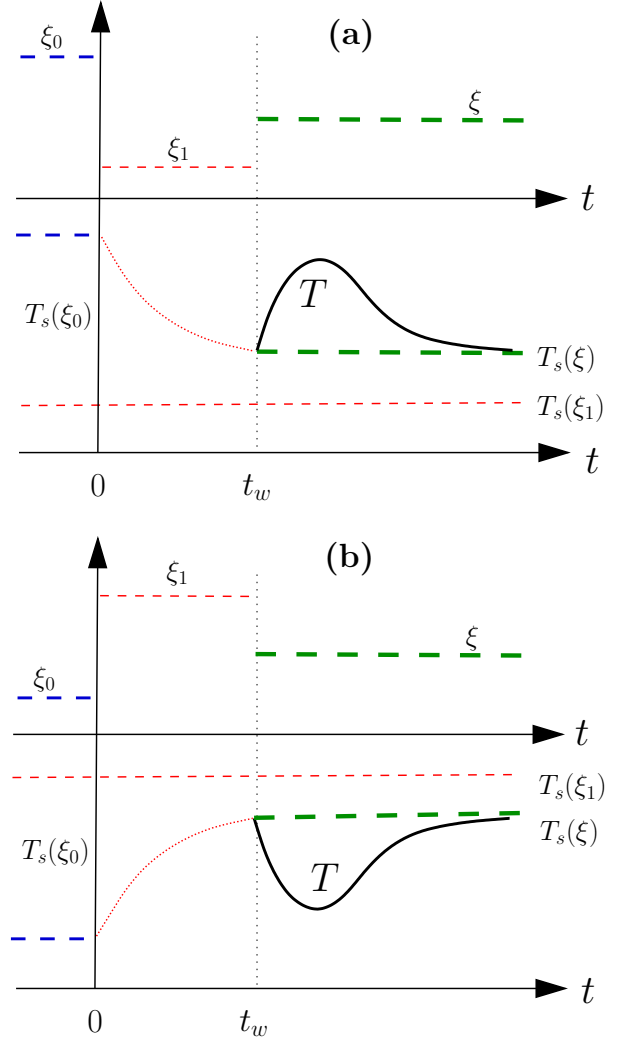


FIG. 1: Sketch of the drive time dependence for the cooling and heated protocols. The resulting *normal* temperature evolution is depicted. The system is first in a non-equilibrium steady state at temperature $T_s(\xi_0)$ under a drive ξ_0 . $T(t_w)$ coincides with $T_s(\xi)$. (a) Cooling protocol: The driving ξ_1 in the waiting time window $0 < t < t_w$ is smaller than its initial value ξ_0 , and the granular temperature would display a maximum before returning to its steady value for $t > t_w$. (b) Heating protocol: We have that $\xi_1 > \xi_0$ and the granular temperature would display a minimum for $t > t_w$.

III. MEMORY EFFECT

We are interested in analyzing the following experiment. First, we let a system of inelastic hard particles reach the steady state corresponding to some value of the driving, say ξ_0 . Then, at $t = 0$ we quench the driving to either $\xi_1 < \xi_0$ (cooling protocol), or to $\xi_1 > \xi_0$ (heating protocol), and the system subsequently evolves for a time t_w , the *waiting time*. At $t = t_w$, we measure the granular temperature and suddenly change the driving to the value ξ such that the stationary granular temper-

ature $T_s(\xi)$ equals the measured value at t_w , $T(t = t_w)$. This amounts to $\xi_1 < \xi < \xi_0$ in the cooling case, and $\xi_1 > \xi > \xi_0$ in the heated one, see Fig. 1. If the state of the system were completely determined by the granular temperature, as is the case in the homogeneous cooling state, the temperature would remain constant for $t > t_w$. But, since the values of the excess kurtosis for $t = t_w$ and for the steady state corresponding to the final driving ξ are different, the granular temperature will separate from its steady value at first, pass through an extremum, and only return to its steady (initial) value for longer times. We may refer to this behavior as the Kovacs hump, because it is similar to the so-called behavior in polymers, structural glasses and other complex systems [25–34].

In the analogous experimental situation for molecular systems, when the “driving” is first lowered ($\xi_0 \rightarrow \xi_1$) and afterwards increased to an intermediate value ($\xi_1 \rightarrow \xi < \xi_0$), the measured quantity, typically the volume [25, 26, 29, 32] or the energy [27, 28, 30, 31, 33, 34], always passes through a maximum. An analogous behavior is expected for any physical quantity that increases with increasing temperature. On the other hand, within the heated protocol, a minimum is expected, as theoretically predicted by linear response theory [31]. Moreover, in the nonlinear regime, the existence of this minimum for the heated protocol has been recently checked for a simple model [33]. We will refer to this behavior, in which the time derivative of the energy changes sign at t_w , that is, the energy displays a rebound, as ‘normal’. It must be stressed here that the final state of the granular gas is not an equilibrium one, but an out-of-equilibrium stationary state, and thus the behavior of the granular temperature may be different.

A. Analytical results

The evolutions in the waiting window ($0 \leq t \leq t_w$), and for $t \geq t_w$ both obey the differential equations (23), but with different initial conditions. At $t = 0$, we have $A_2 = 1$ with either $\beta < 1$ (cooling protocol) or $\beta > 1$ (heating protocol). At $t = t_w$, a ‘reversed’ condition should be enforced, with $\beta = 1$ while A_2 results from the dynamics in the waiting window. $A_2(t_w)$ turns out to be larger than 1 for the cooling protocol, and smaller than 1 in the heated case (see Sec. IV B). Since the waiting time dynamics only enters through the value of $A_2(t_w)$, we assume the latter given, and concentrate on the evolution at $t > t_w$. We shall use the rescaled time τ introduced in (24), with $\tau_w = \zeta_0 \sqrt{T_s} t_w / 2$.

Equations (23) with the initial conditions

$$\beta(\tau = \tau_w) = 1, \quad A_2(\tau = \tau_w) \equiv A_2^{\text{ini}}, \quad (25)$$

do not seem to admit an analytical solution, but an approximate and accurate method can be found in the following way. The initial value of A_2 is of the order of unity: In the cooling case, A_2 is bounded from above by a_2^{HCS}/a_2^s , shown in Fig. 2 and, in the heated case, we

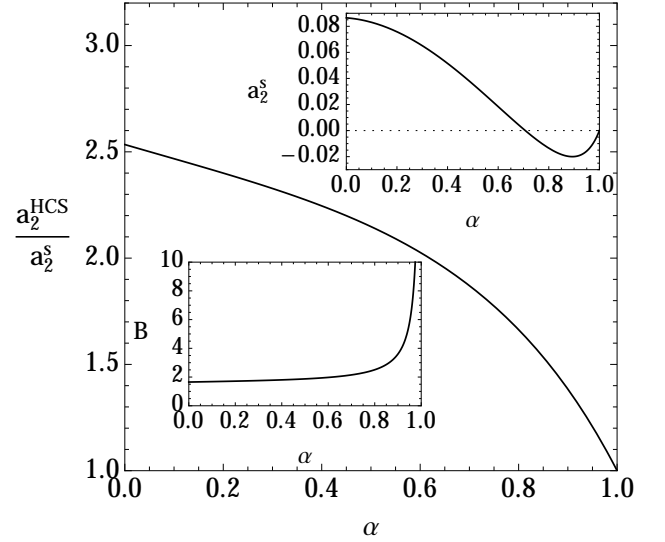


FIG. 2: Plot of a_2^{HCS}/a_2^s as a function of the restitution coefficient α , for a system of inelastic hard disks ($d = 2$), following from the accurate expressions obtained in [12]. The top and bottom insets show the excess kurtosis for the steady state a_2^s and the parameter B as functions of α , as given by Eq. (12) and (17), respectively.

have that $0 < A_2^{\text{ini}} < 1$, as shown in Sec. IV B below. The idea is next to expand both β and A_2 in powers of a_2^s . The rationale for this expansion is the smallness of a_2^s throughout the whole inelasticity range, namely $|a_2^s| \leq 0.086$. Thus we introduce the series expansions

$$\beta(\tau) = \beta_0(\tau) + a_2^s \beta_1(\tau) + \dots, \quad (26a)$$

$$A_2(\tau) = A_{20}(\tau) + a_2^s A_{21}(\tau) + \dots, \quad (26b)$$

into (23), and write the subsequent equations up to linear order in a_2^s . To the zero-th order we have

$$\frac{d\beta_0}{d\tau} = 1 - \beta_0^3, \quad \beta_0 \frac{dA_{20}}{d\tau} = 4 \left[(1 - \beta_0^3) A_{20} + B(1 - A_{20}) \right], \quad (27)$$

submitted to the initial conditions $\beta_0(\tau = \tau_w) = 1$ and $A_{20}(\tau = \tau_w) = A_2^{\text{ini}}$. Therefore, $\beta_0(\tau) = 1, \forall \tau$,

$$\frac{dA_{20}}{d\tau} = -4B(A_{20} - 1). \quad (28)$$

The zero-th order solution is then

$$\beta_0(\tau) = 1, \quad (29a)$$

$$A_{20}(\tau) = 1 + \Delta A_2^{\text{ini}} e^{-4B(\tau - \tau_w)}, \quad \Delta A_2^{\text{ini}} \equiv A_2^{\text{ini}} - 1. \quad (29b)$$

To this order, the granular temperature β_0 remains constant while A_{20} relaxes exponentially from its initial to

its steady state value with a characteristic time (in the τ scale)

$$\tau_c = (4B)^{-1}. \quad (30)$$

There is consequently no memory effect to zeroth order.

The equation for the first order contribution to the scaled temperature is

$$\frac{d\beta_1}{d\tau} = -3\beta_1 + \frac{3}{16}\Delta A_2^{\text{ini}} e^{-4B(\tau-\tau_w)}, \quad \beta_1(\tau = \tau_w) = 0, \quad (31)$$

whose solution is readily obtained as

$$\beta_1(\tau) = \gamma \Delta A_2^{\text{ini}} \left(e^{-3(\tau-\tau_w)} - e^{-4B(\tau-\tau_w)} \right). \quad (32)$$

We have introduced the definition

$$\gamma = \frac{3}{16(4B-3)} > 0, \quad (33)$$

which is positive definite because $B > 3/4$, see Fig. 2. The parameter γ depends on the restitution coefficient α and the dimension of space d , as does B . Note that we have only needed the zero-th order approximation A_{20} for calculating the evolution of the temperature up to first-order in the perturbation parameter a_2^s , that is, β_1 . This stems from the mathematical structure of the equation for β in (23), in which A_2 only appears in the term proportional to a_2^s . We will consider the first-order correction A_{21} to the excess kurtosis in Sec. V, in connection with the long time behavior of the solution.

Equation (32) implies that the sign of $\beta_1(\tau)$ is the same as the sign of $A_2^{\text{ini}} - 1$, which can be shown to be positive for the cooling procedure, and negative in the heated case. We will come back to this feature in Sec. IV B. The time evolution for the temperature, obtained by substituting (29a) and (32) into (26a), is given by

$$\begin{aligned} \beta(\tau) - 1 &= a_2^s \gamma \Delta A_2^{\text{ini}} \left(e^{-3(\tau-\tau_w)} - e^{-4B(\tau-\tau_w)} \right) \\ &= \gamma (a_2^{\text{ini}} - a_2^s) \left(e^{-3(\tau-\tau_w)} - e^{-4B(\tau-\tau_w)} \right), \end{aligned} \quad (34)$$

up to higher order terms in $\mathcal{O}(a_2^s)^2$. Thus, the sign of the “distance” $\beta - 1$ of the granular temperature to its steady value is the same as that of $(a_2^{\text{ini}} - a_2^s)$. If α is changed, it affects both a_2^s and a_2^{ini} so that $(a_2^{\text{ini}} - a_2^s)$ and a_2^s share the same sign, which changes at a certain value of the restitution coefficient, $\alpha_c \simeq 1/\sqrt{2} \simeq 0.707$ [43]: as a consequence, $a_2^s > 0$ for $\alpha < \alpha_c$ while $a_2^s < 0$ for $\alpha > \alpha_c$, see the top inset in Fig. 2. We now restrict the discussion to cooling protocols. The above reasoning implies that for high inelasticities, namely $\alpha < \alpha_c$, $\beta - 1 > 0$ and then β has a maximum while the granular temperature has a minimum (remember that $T = T_s/\beta^2$). The situation reverses for small inelasticities, $\alpha > \alpha_c$, for which $\beta - 1 < 0$. Then, β has a minimum, which corresponds to a maximum of the granular temperature. On the other hand,

for heating protocols, the phenomenology is reversed, but ruled by very similar mechanisms. For $\alpha > \alpha_c$, T shows a minimum, whereas for $\alpha < \alpha_c$, it exhibits a maximum. A more physical explanation will be provided in subsection IV A.

It should be noted here that from the structure of Eq. (34), the shape of the hump (the τ dependence) and its amplitude are factorized. In other words, Eq. (34) can be rewritten as

$$\beta(\tau) - 1 = g(\tau_w) h(\tau - \tau_w), \quad (35a)$$

$$g(\tau_w) = a_2^s \Delta A_2^{\text{ini}} = a_2^{\text{ini}} - a_2^s, \quad (35b)$$

$$h(s) = \gamma (e^{-3s} - e^{-4Bs}) > 0. \quad (35c)$$

The prefactor $g(\tau_w)$ contains all the information about the details of the protocol in the waiting time window, that is, the dependence of the hump not only on t_w but also on $\{\xi_0, \xi_1\}$, while $h(\tau - \tau_w)$ determines its shape. We shall show in Sec. IV B that ΔA_2^{ini} has a definite sign for both cooling and heating protocols, so that g also determines the sign of the hump through the steady value of the excess kurtosis a_2^s or, equivalently, $a_2^{\text{ini}} - a_2^s$.

Equation (34) or (35) gives then the lowest order expression for the Kovacs hump, within the theoretical framework we have just developed. It clearly shows that the granular temperature is not enough for describing the state of uniformly heated granular gases, as has been already claimed by other means [16, 17]. If that were the case, no hump at all would be present when the system is prepared with the *correct* initial granular temperature for the subsequent driving, within our à la Kovacs program. On the other hand, the existence of the Kovacs hump does not directly follow from the non-Maxwellian character of the velocity distribution. Indeed, although the velocity distribution of a granular gas is generically non-Gaussian, the granular temperature may completely specify its state in some situations. This is the case for the homogeneous cooling state but also for the equivalent system driven by the so-called Gaussian thermostat. Therein, particles are accelerated between collisions by a force proportional to their own velocity [11, 35, 36], and no Kovacs hump would be observed if an analogous stepwise driving procedure were followed.

B. Numerical results

We compare here the analytical expression for the Kovacs hump to the results obtained by direct Monte Carlo simulations [44] of the Boltzmann-Fokker-Planck equation. We have used a system of $N = 10^4$ hard disks ($d = 2$) of unit mass, $m = 1$, and unit diameter, $\sigma = 1$, with the collision rule (1). The results have been averaged over a large number (ranging from $N_T = 10^5$ to 1.5×10^6) of realizations of the stochastic dynamics of the system. The stochastic thermostat is taken into account by the procedure first introduced in Ref. [10]. Over each trajectory, the hard disks are submitted to random kicks

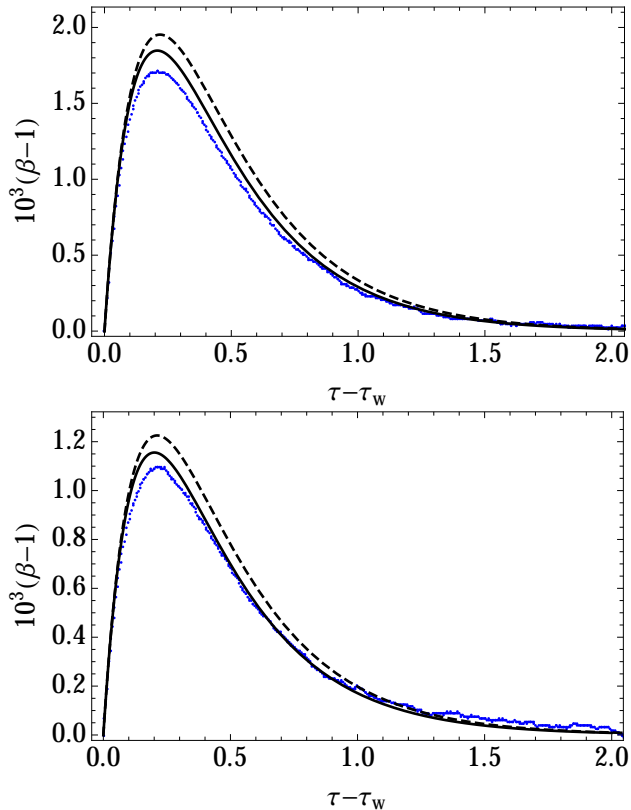


FIG. 3: Plot of the Kovacs hump for $\alpha = 0$ (top) and $\alpha = 0.3$ (bottom). The simulation curves (points) have been averaged over 10^5 trajectories, and they are compared to (i) the *raw* theoretical curve (34), evaluated with the theoretical expressions for the parameters a_2^s , B , and a_2^{HCS} (dashed line) and (ii) the improved theory obtained by inserting into (34) the value of the B -parameter given by the Monte Carlo simulation (solid line). The second route improves the agreement between theory and simulation. The specific values of the parameters for each of the plotted curves are given in Table I. Note the smallness of $\beta - 1$, which is of the order of 10^{-3} in both cases.

every $N_c = N/10^3 = 10$ collisions. In the kick, each component of the velocity of every particle is incremented by a random number extracted from a gaussian distribution of variance $\xi^2 \Delta t$, where Δt is the time interval corresponding to the number of collisions N_c . Moreover, every $N/10^2 = 100$ collisions, a possible non-vanishing center of mass velocity is eliminated to enforce conservation of momentum and avoid a spurious drift of the center-of-mass velocity.

Our analytical predictions reveal that the Kovacs effect is all the more pronounced as the difference $|a_2^{\text{ini}} - a_2^s|$ is large. Quite intuitively, there are two ways to maximize $|a_2^{\text{ini}} - a_2^s|$: either taking $\xi_1 \ll \xi_0$ (equivalently $T_s(\xi_1) \ll T_s(\xi_0)$ in the cooling case, or in the heated situation, reversing all inequalities. We concentrate here on the cooling protocol, for which we have performed simulations such that the choice $\xi_1 \ll \xi_0$ guaranties that the system, in the waiting time window, has an excess kur-

	$\alpha = 0$	$\alpha = 0.3$	$\alpha = 0.8$
B from DSMC	1.802	1.920	2.440
B from (17)	1.422	1.555	2.602
B from (21)	1.652	1.753	2.507

TABLE I: Values of the excess kurtosis decay rate B , corresponding to the plots in Figs. 3 and 5. For comparison with Monte Carlo data, Eq. (21) has been used.

tosis that quickly evolves towards its free cooling counterpart; thus, $A_2(\tau_w) = a_2^{\text{HCS}}/a_2^s$. We will discuss in subsection IV B the cases of finite ξ_1/ξ_0 . For the sake of simplicity, we have always used $\xi_1 = 0$, which allows us to simplify the simulation procedure, see below.

Let us explain how we calculate in the simulations the final value of the driving ξ from the value of the granular temperature $T(t_w)$ at the end of the waiting time window. For an arbitrary value of the intermediate driving ξ_1 : (i) run all the realizations until the waiting time, (ii) obtain the granular temperature $T(t_w)$ averaging over all the realizations, (iii) determine the final value of the driving ξ therefrom, and (iv) continue running all the realizations. This numerical procedure introduces some (in general unavoidable) numerical errors, stemming from the fluctuations of the granular temperature over the different realizations. Nevertheless, we may take advantage of the value of the driving in the waiting time window, $\xi_1 = 0$, to eliminate these fluctuations and minimize the numerical error. For long enough waiting times [45], the system cools in the homogenous cooling state, a regime where all the time evolution may be encoded in the granular temperature. Then, we proceed in the following way: (i) We choose a value of the final driving ξ , and calculate the corresponding steady granular temperature $T_s(\xi)$, (ii) run each realization until the shortest time t such that $T(t) < T_s(\xi)$, (iii) rescale all the velocities of the particles with a factor $\sqrt{T_s(\xi)/T(t)}$, so that $T(t) = T_s(\xi)$, thus effectively eliminating the granular temperature fluctuations at the waiting time, and (iv) continue running all the realizations.

In Fig. 3, we show the comparison between the numerical computation of the Kovacs hump and our theoretical prediction, in the high inelasticity regime $\alpha < \alpha_c \simeq 0.707$. Namely, we have considered (a) $\alpha = 0$ and (b) $\alpha = 0.3$. In both cases, there are two theoretical curves: the dashed line corresponds to the raw evaluation of Eq. (34) with the theoretical values of a_2^s , a_2^{HCS} and B given by Eqs. (12), (18) and (21), respectively. Although the qualitative agreement is reasonable, there are quantitative discrepancies. This is not surprising. While the analytical predictions for a_2^s and a_2^{HCS} turn out reliable for our purposes, Eq. (21) does not fare as well, and may be plagued by nonlinear effects, as is the case for Eq. (17) [16]. Therefore, we have followed an alternative route: We first measure B from the relaxation of the excess kurtosis, as embodied in relation (29b), see Fig. 4, which clearly exhibits an exponential behavior. The cor-

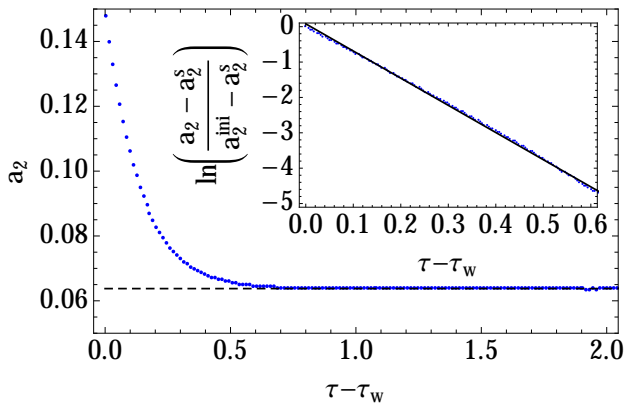


FIG. 4: Decay of the excess kurtosis from its initial to its steady state value. Plotted is the simulation curve obtained by DSMC (points) for $\alpha = 0.3$. The long time limit is very close to its predicted value $a_2^s = 0.00638$, following from Eq. (12) and shown by the dashed line. In the inset, the same decay but on a logarithmic scale (points). From the linear slope, we directly measure the parameter B , to be inserted into the theoretical expression for the Kovacs hump, Eq. (34). The obtained values are given in Table I.

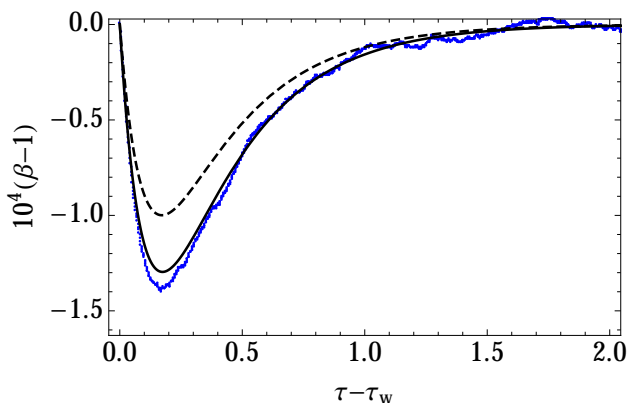


FIG. 5: Plot of the Kovacs hump for $\alpha = 0.8$. The meaning of the different symbols and lines is the same as in Fig. 3. Note that the sign of $\beta - 1$ is reversed, $\beta - 1 < 0$ as the restitution coefficient $\alpha > \alpha_c \simeq 0.707$.

responding value of B is then inserted in Eq. (34), to give the solid line in Fig. 3. A posteriori, we have also compared the values of B to their analytical counterparts, as seen in Table I. The inaccuracy of the theoretical estimate is of approximately 10% for Eq. (21), and 20% with Eq. (17), consistently with the situation found in previous studies [16]. It appears that once an accurate value of the relaxation parameter B is known, quantitative predictions can be made.

Figure 5 shows the Kovacs hump for a smaller value of the inelasticity, namely $\alpha = 0.8 > \alpha_c$. As predicted by the theory, the sign of $\beta - 1$ is reversed, since $a_2^s < 0$ for $\alpha > \alpha_c$. The simulation curve has been averaged over 1.5×10^6 trajectories, because in this region not only $|a_2^s|$ but also ΔA_2^{ini} are of smaller magnitude, see Fig. 2. Thus,

the amplitude of the hump is reduced roughly tenfold as compared to those in Fig. 3. For $\alpha = 0.8$, the error in the theoretical estimate of $(a_2^{\text{HCS}} - a_2^s)$ is of the order of 20 per cent, roughly an order of magnitude larger than the one for the highly dissipative cases of Fig. 3. Therefore, in order to obtain a good agreement between theory and simulation (solid line), we have to insert into (34) both the measured value of B and the simulation value of the excess kurtosis difference $(a_2^{\text{HCS}} - a_2^s)$ [46]. A similar situation, in which not only B but also the excess kurtosis had to be taken from the simulations, was found in the analysis of the universal reference state of Ref. [16] in the same range of inelasticities.

IV. SIGN AND MAGNITUDE OF THE EXTREMUM

A. Physical origin of the effect

We attempt here a more physical explanation of the mechanism at work here, which is, expectedly, very different from that in glassy systems. In essence, the effects we observe are subtle consequences of energy dissipation. Without loss of generality, we focus on the cooling protocol. An important feature is the shape of the velocity distribution $f(\mathbf{v}, t)$, through the sign of the excess kurtosis a_2 . Is it “flatter” than the Gaussian (so-called platykurtic, with $a_2 < 0$), or is it “thinner” (so-called leptokurtic, with $a_2 > 0$)? *Distributions with $a_2 < 0$ dissipate less energy* (and conversely, more energy when $a_2 > 0$). Indeed, one can show that to linear order in the excess kurtosis,

$$\frac{\langle v_{12}^n \rangle}{\langle v_{12}^n \rangle_0} = 1 + a_2 \frac{n(n-2)}{16}, \quad (36)$$

where the average with index 0 refers to a Gaussian distribution of the same variance, and v_{12} is the modulus of the relative velocity. The correction to unity vanishes when $n = 0$ (normalization) and $n = 2$ (equality of variances). Energy dissipation is related to the moment $n = 3$ (one v coming from the collision frequency, and a v^2 from the fact that we are interested in the kinetic energy). Thus $\langle v_{12}^3 \rangle < \langle v_{12}^3 \rangle_0$, for $a_2 < 0$ [47].

We start by discussing the behavior of the system in the cooling protocol, see Fig. 1 (a), in which the driving in the waiting time window is smaller than the initial one, $\xi_1 < \xi_0$. Moreover, and for the sake of simplicity, we focus in the limiting case $\xi_1 = 0$, in which the system freely cools for $0 < t < t_w$. We analyze the case $\xi_1 \neq 0$ in Sec. IV B, in which we show that this change only affect the magnitude of the effect, but not its sign. Close to elasticity, $a_2 < 0$, for both driven and undriven gases (platykurtic behavior). It is quite difficult to shape an intuition for the sign. It may be tempting to argue that it is a means for the system to minimize energy dissipation, in spite of the lack of a general principle holding for such non-equilibrium systems. What is more intuitive is

that the unforced system shows stronger non Gaussianities than the driven one, which benefits from stochastic kicks from the forcing, $|a_2^{\text{HCS}}|/|a_2^s| > 1$. Hence, at $t = t_w$, the system is in a state where a_2 is more negative than it asymptotically will be, and therefore, energy dissipation is, transiently, less. This implies that T shows a maximum (or β a minimum, as we observe).

The above scenario applies as long as dissipation is not too large ($\alpha > \alpha_c = 1/\sqrt{2}$). On the other hand, for $\alpha < \alpha_c = 1/\sqrt{2}$, the driven and undriven systems become leptokurtic ($a_2 > 0$, in order, in a hand-waving fashion, to cope with large dissipation). We can subsequently follow the same reasoning as above, which explains the anomalous effect. The undriven kurtosis is larger than the driven one (the driven f is always the most Gaussian), so that the larger value of a_2 at t_w brings extra dissipation. Thus, T shows an undershooting (maximum of β).

For heating protocols, see Fig. 1(b), we next focus on the limiting case $\xi_1 \rightarrow \infty$. Again, a finite value of the driving in the waiting time window ξ_1 does not change the sign of the effect but only its magnitude, see next section. For a very large value of ξ_1 , the system rapidly evolves to a gaussian distribution with $a_2 = 0$ in the waiting time window. Therefore, we always have that $|a_2^s| > |a_2^{\text{ini}}| = 0$ and following the same line of reasoning as in the cooling case, it is easily shown that the separation of the temperature from its steady value is simply reversed.

The above picture remains valid for a closely related thermostat, in which the energy injection is the same but the bath provides an additional friction force [48]. In particular, the value of the excess kurtosis for that thermostat also verifies that $|a_2^s| < |a_2^{\text{HCS}}|$. The introduction of this additional friction force allows the system to reach a well-defined steady state even in the elastic limit $\alpha = 1$, in which the dissipation stemming from collisions disappears.

B. The optimal waiting time

We now return to the cooling protocol, in the limiting case where ξ_1/ξ_0 is close to zero. At $\xi_1/\xi_0 = 0$, the waiting time t_w can be arbitrarily large, since a_2 will evolve to a_2^{HCS} , and the longer one waits (in real time scale, not in the τ scale, see below), the stronger the effect. In general however, there is an optimal value of t_w , which depends on the ratio $T_s(\xi_1)/T_s(\xi_0)$, for which the amplitude of the Kovacs response is maximal. The reason is that the difference in kurtosis, $|a_2(t_w) - a_2^s|$, should be maximized. If one spends too much time in the waiting window, the system can attain its non-equilibrium steady state, $a_2(t_w)$ then reaches the value a_2^s ($A_2 \rightarrow 1$), and the humps disappears. This holds for both the cooling ($\xi_1 < \xi_0$) and the heated ($\xi_1 > \xi_0$) protocols, see Figures 6, 7 and 8. These figures therefore exhibit an extremum at a particular value of τ_w , which provides the optimal waiting time. It can be observed that in the τ scale, this

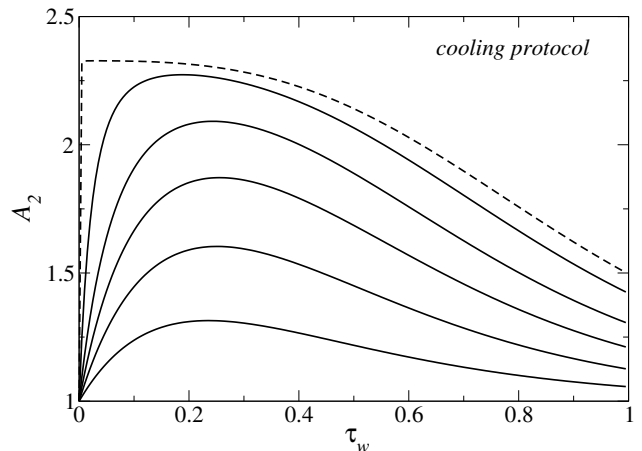


FIG. 6: Evolution of excess kurtosis ratio, $A_2(\tau_w) \equiv a_2(\tau_w)/a_2^s$, as a function of waiting time, within the cooling protocol at $\alpha = 0.3$. From bottom to top, the curves correspond to $T_s(\xi_0)/T_s(\xi_1) = 2, 4, 9, 25$ and 200. The upper dashed curve is for the limit $T_s(\xi_1)/T_s(\xi_0) \rightarrow 0$. Note that $A_2(\tau_w)$ defines the quantity A_2^{ini} used throughout. For a given value of α , the maximum possible A_2 is a_2^{HCS}/a_2^s . For $\alpha = 0.3$, Fig. 2 indicates that this ratio is close to 2.33, which is consistent with the maximum of the dashed curve.

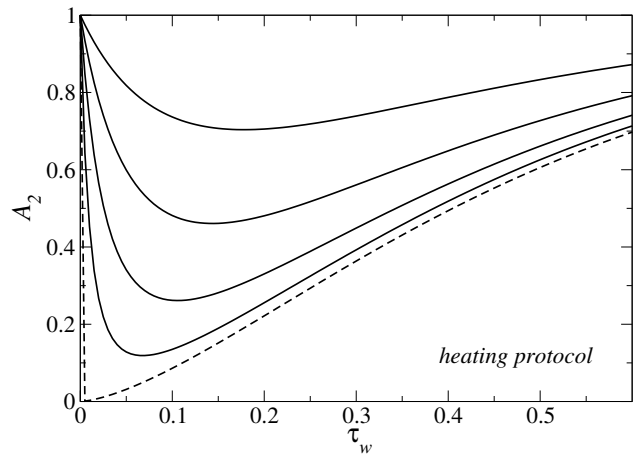


FIG. 7: Same as Fig. 6 but for the heated protocol. Here, from top to bottom: $T_s(\xi_1)/T_s(\xi_0) = 2, 4, 9, 25$. The lower dashed curve is for $T_s(\xi_1)/T_s(\xi_0) \rightarrow \infty$

optimum depends only weakly on ξ_1/ξ_0 (or equivalently on $T_s(\xi_1)/T_s(\xi_0)$), and likewise, quite weakly on dissipation.

The trends observed in the Figures, with a maximum (resp. minimum) in the cooling (resp. heating) case, can be understood as in Sec. IV A, and are fully consistent with the argument put forward there. In the extreme case $T_s(\xi_1)/T_s(\xi_0) \rightarrow \infty$ (that is, $\xi_1/\xi_0 \rightarrow \infty$), the velocity distribution is provided enough time to become Gaussian, with thus a vanishing a_2 (and A_2). This is the behavior shown in Fig. 7. Yet, the dashed line also shows that for any finite $T_s(\xi_1)/T_s(\xi_0)$, no matter how large, the optimal waiting time becomes vanishingly small in the τ

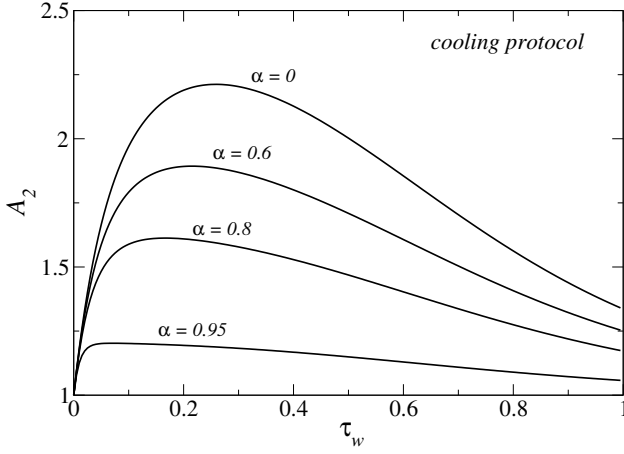


FIG. 8: Excess kurtosis ratio as a function of waiting time (cooling protocol), for different dissipations, and $T_s(\xi_1)/T_s(\xi_0) = 1/25$.

scale, which reflects the fact that under extreme forcing ξ_1 , the system is so much driven that it is able to quickly reach its steady-state. It is at this point interesting to turn to the dashed line in Fig. 6 for the cooled extreme case $\xi_1/\xi_0 \rightarrow 0$. It also reveals that the optimal τ_w also vanishes, whereas, on intuitive grounds, it should be that one can wait arbitrarily long without seeing the system depart from the homogeneous cooling state it quickly attains. In other words, one may expect that the optimal waiting time should diverge upon decreasing the forcing. This is the case, but it can only be appreciated by returning to the original t scale: it turns out that the optimal $t_w \propto \tau_w/\sqrt{T_s(\xi_1)}$ diverges when $\xi_1 \rightarrow 0$, due to the vanishing of $T_s(\xi_1)$.

We attempt here a summary of the main results reported in this Section. The Kovacs-like protocol used throughout this paper can be described by three dimensionless parameters: (i) the restitution coefficient α , (ii) the ratio ξ_1/ξ_0 of the intermediate driving ξ_1 to the initial one ξ_0 , and (iii) the dimensionless waiting time τ_w , which in turn fixes the ratio ξ/ξ_1 . The sign of the hump is completely determined by the first two, α and ξ_1/ξ_0 , while the third only affects the magnitude of the extremum. A *phase diagram* of the Kovacs hump is sketched in Fig. 9. The “normal” behavior is similar to the one observed in molecular systems when controlling the bath temperature and measuring the energy (or the volume). The lines in the diagram indicate the values of the parameters for which no Kovacs hump would be observed. The solid line $\xi_1 = \xi_0$ separating heating and cooling protocols delineates a “trivial” boundary, with no change in the driving and thus no hump. On the other hand, the dashed line $\alpha = \alpha_c$ separating the low and high inelasticity regions is less expected, and follows from the accurate prediction of the first Sonine approximation for the change of sign in the Kovacs hump.

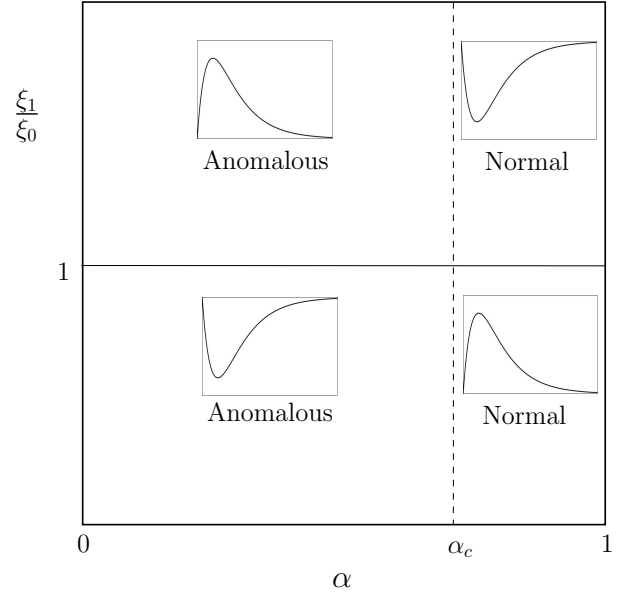


FIG. 9: Phase diagram of the Kovacs hump. The line $\xi_1/\xi_0 = 1$ (solid) separates the “cooling” ($\xi_1 < \xi_0$) and the “heating” ($\xi_1 > \xi_0$) protocols. The dashed line $\alpha = \alpha_c = 1/\sqrt{2}$ separates systems with “high inelasticity” ($\alpha < \alpha_c$) from those with “low inelasticity” ($\alpha > \alpha_c$). Note that the plots are for the granular temperature T , a maximum in T corresponds to a minimum in the β variable defined in Eq. (14).

V. LONG TIME BEHAVIOR AND COMPATIBILITY WITH THE UNIVERSAL REFERENCE STATE

On close inspection, the trends reported above for the time evolution of β are not compatible with the requirement that the system should asymptotically evolve towards the universal state brought to the fore in Ref. [16]. We discuss and resolve that question here. In a nutshell, the time evolution is slightly more complex than the simplified expressions obtained in Section III A. For the sake of simplicity, we use in this section the shifted time variable $\tau = \zeta_0\sqrt{T_s}(t - t_w)/2$, which vanishes at $t = t_w$. Let us consider the equation for the first-order correction to the excess kurtosis,

$$\frac{dA_{21}}{d\tau} + 4BA_{21} = -[(12 - 4B)A_{20} + 4B]\beta_1. \quad (37)$$

We do not write here its complete solution, but only its leading behavior for long times. The solution of (37) is a linear combination of exponentials with different relaxation times. For $\tau \rightarrow \infty$, the rhs of (37) behaves, to dominant order, as

$$h(\tau) = -12\gamma\Delta A_2^{\text{ini}}e^{-3\tau}, \quad (38)$$

as follows from Eq. (29b) and (32). The term in A_{21} coming therefrom is

$$A_{21}^h(\tau) = -64\gamma^2\Delta A_2^{\text{ini}}e^{-3\tau}, \quad (39)$$

and asymptotically dominates

$$A_{21}(\tau) \sim A_{21}^h(\tau), \quad \tau \gg 1. \quad (40)$$

Interestingly, this term is much bigger than $A_{20}(\tau)$ for very long times, and thus gives the long time tendency to the steady value of the rescaled excess kurtosis,

$$A_2(\tau) - 1 \sim a_2^s A_{21}^h(\tau), \quad \tau \gg 1. \quad (41)$$

The condition for the asymptotic result in (41) to hold is, more concretely, $\exp(-4B\tau) \ll \exp(-3\tau)$ or, equivalently, $\exp[-(4B-3)\tau] \ll 1$. It is worth noting that the sign of $A_{21}^h(\tau)$ is opposite to that of ΔA_2^{ini} and therefore different from that of the zero-th order contribution $A_{20}(\tau) - 1$, see Eq. (29b). As $a_2^s < 0$ for weakly dissipative systems, $\alpha > \alpha_c$ while $a_2^s > 0$ in the highly dissipative case, $\alpha < \alpha_c$, Eq. (41) predicts that, for long times $\tau \gg 1$, the sign of $A_2 - 1$ is the opposite to that of $A_{20} - 1$ for $\alpha < \alpha_c$. This means that A_2 has a minimum and tends to unity from below in the highly dissipative case. This behavior was overlooked by the analysis performed in previous sections. The effect is quite small and thus difficult to measure in the simulations, but it has important theoretical consequences. In Ref. [16] it was proved that, for long enough times, a uniformly heated granular gas reaches the *universal reference β -state*, over which all the time dependence can be encoded in β . In other words, for long enough times, all the moments of the velocity distribution function (for instance, the excess kurtosis) forget their initial conditions and become only a function of the “distance” β to the steady state. Afterwards, for even longer times, β approaches its steady value. For the excess kurtosis, and in the linear regime close to the steady state, this universal behavior is given by

$$A_2 - 1 \sim \left. \frac{dA_2}{d\beta} \right|_{\beta=1} (\beta - 1) = -\frac{12}{4B-3}(\beta - 1). \quad (42)$$

The value of the derivative $dA_2/d\beta|_{\beta=1}$ has been calculated by applying L'Hôpital rule to Eq. (19) of Ref. [16].

If we take the lowest order approximation for both $A_2 - 1$, which is $A_{20} - 1$, and for $\beta - 1$, which is given by β_1 , we have that

$$\lim_{\tau \rightarrow \infty} \frac{A_{20} - 1}{\beta - 1} = 0, \quad (43)$$

in strong disagreement with (42), which predicts a value $-12/(4B-3) < 0$ instead. This problem is mended if we consider, as should be done, $A_2 - 1$ and $\beta - 1$ up to the same order. Since the dominant term for long times in the decay of A_2 is proportional to A_{21}^h , as given by (41), and the long time behavior of $\beta - 1$ can be straightforwardly inferred from (34),

$$\beta(\tau) - 1 \sim a_2^s \gamma \Delta A_2^{\text{ini}} e^{-3\tau}, \quad (44)$$

one obtains that

$$\frac{A_2 - 1}{\beta - 1} \sim -64\gamma = \frac{-12}{4B-3}, \quad \tau \gg 1, \quad (45)$$

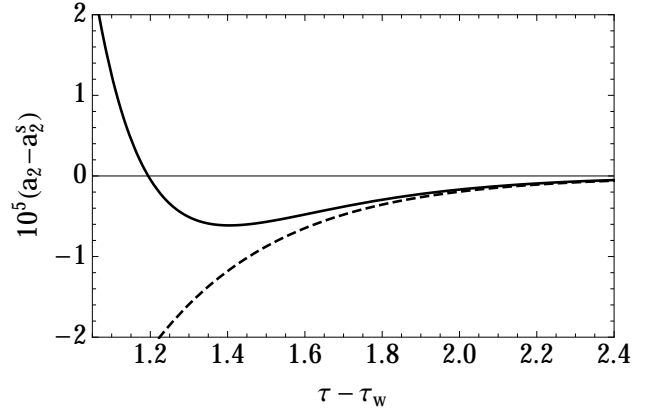


FIG. 10: Tendency to the universal reference state for very long times. We show a zoom of the long time behavior ($\tau - \tau_w \geq 1$) of the decay of the excess kurtosis to its steady value, $|a_2 - a_2^s| \leq 2 \times 10^{-5}$. The overall picture is that of Fig. 4, which also corresponds to $\alpha = 0.3$, for which $a_2^{\text{ini}} - a_2^s \simeq 0.086$. Plotted here is the excess kurtosis decay obtained from (i) the numerical integration of Eq. (23) with initial conditions (25) (solid line) (ii) the asymptotic behavior given by Eq. (41) and (39) (dashed line).

where the definition of γ , Eq. (33), has been used. The result in (45) is in agreement with (42).

Figure 10 shows the tendency of the system to approach the universal reference state for very long times. Although to the zero-th order the overall relaxation of the excess kurtosis to the steady state is very well described by a single exponential, see Fig. 4, for very long times $a_2 - a_2^s$ changes sign and tends to zero from below. This is in full agreement with the approach to the universal reference state, as described by Eq. (42) or (45). The minimum is tiny, being four orders of magnitude smaller than the initial distance to the steady state for the plotted case ($\alpha = 0.3$). This makes it very difficult to measure this effect in simulations. However, it is crucial from a theoretical point of view, since it shows that the theoretical approach developed here is compatible with the general long time behavior derived in Ref. [16].

VI. FINAL REMARKS

In conclusion, we have studied from a granular gas perspective a memory effect that pertains to glassy phenomenology. A striking consequence of the analysis is that the sign of the Kovacs hump changes as the restitution coefficient is varied from the quasi-elastic limit $\alpha \rightarrow 1^-$ to the completely inelastic case $\alpha = 0$. There is a critical value of the restitution coefficient α_c , which coincides with the point at which the stationary value of the excess kurtosis changes sign. First, we recapitulate the behavior for cooling protocols as the one depicted in Fig. 1(a). For weakly dissipative systems, in the sense that $\alpha > \alpha_c$, the granular temperature passes through a

maximum, larger than its corresponding steady value T_s ($\beta = \sqrt{T_s/T} < 1$). The sign of the hump changes for highly dissipative systems, in which $\alpha < \alpha_c$: the temperature passes through a minimum ($\beta > 1$). Conversely, for heating protocols, in which $\xi_0 < \xi < \xi_1$ as sketched in Fig. 1(b), we simply have a reversal of the sign of the hump: the granular temperature displays a minimum for small inelasticity, $\alpha > \alpha_c$ and a maximum for high inelasticity $\alpha < \alpha_c$. Table II summarizes the phenomenology. On the other hand, in a molecular system, the measured quantity in the analogous experimental situation [49] always exhibits a maximum (resp. minimum) in the cooling (resp. heating) protocol. This stems from the mathematical structure of the analytical expression for the Kovacs hump within linear response theory, but the same result seems to remain valid in the nonlinear regime [31, 33, 34].

Therefore, the Kovacs effect for uniformly heated granular gases is *normal* for small inelasticities while it is *anomalous* in the highly inelastic case, independently of the details of the protocol followed in the waiting time window. The intermediate value of the driving ξ_1 and the waiting time t_w do affect the amplitude of the memory effect, but not its sign and shape, as expressed by Eq. (35) and discussed in Sec. IV. Nevertheless, there are optimal values of ξ_1 and t_w that maximize the amplitude of the hump for a given value of the restitution coefficient. Quite intuitively, for the usual cooling protocol the optimal choice of parameters corresponds to the limit $\xi_1 \rightarrow 0$ with a large enough t_w , such that the system ends up in the homogeneous cooling state inside the waiting time window.

In molecular systems, energy is conserved and, within the linear response regime, the shape of the Kovacs hump is closely related to the linear relaxation function of the energy from the initial temperature T_0 to the final one T . This *direct* relaxation function decays monotonically because it is proportional to the equilibrium time autocorrelation function of the energy, as stated by the fluctuation-dissipation theorem [50]. In turn, this monotonicity assures that the Kovacs hump is always positive for the usual cooling protocol [31], while it is negative for the heating protocol considered in Ref. [33]. Therefore, it seems worth investigating the anomalous character of the Kovacs hump found here for high dissipation. Specifically, it would be interesting to analyze the possible relation between the anomalous character of the Kovacs effect for high dissipation and the validity of the fluctuation-dissipation relation in non-equilibrium systems. In the context of granular media, there is some recent work trying to establish the validity of fluctuation-dissipation relations. [13, 51–55]. It seems particularly appealing to investigate simple models of dissipative systems [53, 56], for which the calculations may be carried out without introducing any approximations like the Sonine expansion considered here.

Our main assumptions are (i) the accurateness of the first-Sonine approximation (ii) the smallness of the excess kurtosis that makes it possible to neglect nonlinear

terms in a_2 . Our expression for the Kovacs hump, as given by Eq. (34), is valid up to the linear order in the excess kurtosis. If nonlinear corrections in a_2 were incorporated to the time evolution equations, this linear order result would not be affected. The exponential decay of the excess kurtosis to the zero-th order, as given by A_{20} , is neither affected by the introduction of nonlinearities. The same is applicable to the long time behavior and the tendency to the universal reference state discussed in Sec. V. This may be surprising at first sight, because nonlinearities in a_2 should certainly change the equation for the excess kurtosis first-order correction A_{21} . However, these nonlinearities must vanish in the steady state (as $(A_2 - 1)^2$ to the quadratic order), and thus they are subdominant against the leading term as given by $h(\tau)$, Eq. (38). The results derived throughout the paper are therefore robust.

One of the main implications of the original work by Kovacs is that it clearly showed that the experimental macroscopic variables (pressure, volume, temperature, for polymers) do not suffice to completely characterize the system state, which in general depends on the whole previous thermal history. In this sense, the existence of the Kovacs hump here, independently of its amplitude and sign (normal or anomalous), is a crisp proof that the state of the uniformly heated granular gas is not uniquely determined by its granular temperature, and other variables must be incorporated to have a complete description thereof. At first glance, this conclusion seems similar to that reached in the analysis of its universal reference β -state [16, 17], in which it was shown that the “distance” to the steady state β is also necessary to describe the uniformly driven granular gas. But it must be stressed that here, we go further. While the β -state reached for long times is uniquely determined by the driving ξ and the granular temperature T , we show the relevance of explicitly keeping track of the intrinsic dynamics of non-Gaussianities, through the decoupling of a_2 and β .

In principle, a similar behavior should appear for other kinds of drivings, provided that the driving intensity and the granular temperature do not suffice to completely characterize the state of the system. Within the first Sonine approximation, the magnitude of the Kovacs hump would be proportional to the difference between the initial value of the excess kurtosis a_2^{ini} and its steady value for the considered thermostat [57]. In the usual cooling protocol, if a very low value of the intermediate driving ξ_1 were used, the value of the excess kurtosis after the waiting time would be close to that of the homogeneous cooling state. Therefore, non-Gaussianities are a necessary but not sufficient condition to have memory effect of the kind reported here in a driven granular gas [58]. In all generality, the possibility of having a transition from normal to anomalous Kovacs effect is encoded in the change of sign of $a_2^{\text{ini}} - a_2^s$.

The Kovacs hump in granular gases occurs over the kinetic time scale. For the time at which the temperature passes through its extremum, the system has not

protocol	inelasticity	α	$a_2^{\text{ini}} - a_2^{\text{s}}$	dissipation	T hump	Kovacs effect
cooling	“low”	$> \alpha_c$	< 0	smaller than stationary	maximum	normal
cooling	“high”	$< \alpha_c$	> 0	larger than stationary	minimum	anomalous
heating	“low”	$> \alpha_c$	> 0	larger than stationary	minimum	normal
heating	“high”	$< \alpha_c$	< 0	smaller than stationary	maximum	anomalous

TABLE II: Hump phenomenology and the underlying physical mechanism for the cooling and heating driving protocols in Fig. 1. The ‘critical’ value of the restitution coefficient α is $\alpha_c = 1/\sqrt{2}$.

reached the *hydrodynamic* stage [59] in which the all the time dependence of the velocity distribution function occurs through the hydrodynamic fields (density, average velocity and temperature), and initial conditions have been forgotten. Over the hydrodynamic β -state of uniformly driven gases, the decay of the temperature (or of β) to its steady value is a monotonic function of time [16, 17]. Here, this monotonicity condition is only fulfilled for times greater than that of the extremum. Then, the system reaches this hydrodynamic solution of the Boltzmann equation only for very long times, when it is linearly close to the steady state.

Acknowledgments

We acknowledge useful discussions with M.I. García de Soria and P. Maynar. This work has been supported by the Spanish Ministerio de Economía y Competitividad grant FIS2011-24460 (AP). AP would also like to thank the Spanish Ministerio de Educación, Cultura y Deporte mobility grant PRX12/00362 that funded his stay at the Université Paris-Sud in summer 2013, during which this work was carried out.

-
- [1] H. Jaeger, S. R. Nagel, and R. Behringer, Rev. Mod. Phys. **68** 1259 (1996).
 - [2] A. Barrat, E. Trizac, and M. H. Ernst, J. Phys.: Condens. Matter **17**, S2429 (2005).
 - [3] T. Pöschel and N. Brilliantov eds., *Granular Gas Dynamics*, (Springer, Berlin, 2003).
 - [4] N. Brilliantov and T. Pöschel, *Kinetic Theory of Granular Gases* (Clarendon Press, Oxford, 2004).
 - [5] A. Goldshtein and M. Shapiro, J. Fluid. Mech. **282**, 75 (1995).
 - [6] J. J. Brey, M. J. Ruiz-Montero, and D. Cubero, Phys. Rev. E **54**, 3664 (1996).
 - [7] T. P. C. van Noije, and M. H. Ernst, Granular Matter **1**, 57 (1998).
 - [8] P. K. Haff, J. Fluid. Mech. **134**, 401 (1983).
 - [9] D. R. M. Williams and F. C. MacKintosh, Phys. Rev. E **54**, R9 (1996).
 - [10] T. P. C. van Noije, M. H. Ernst, E. Trizac, and I. Pagonabarraga, Phys. Rev. E **59**, 4326 (1999).
 - [11] J. M. Montanero and A. Santos, Granular Matter **2**, 53 (2000).
 - [12] A. Santos and J. M. Montanero, Granular Matter **11**, 157 (2009).
 - [13] P. Maynar, M.I. García de Soria, and E. Trizac, Eur. Phys. J. Special Topics **179**, 123 (2009).
 - [14] M. H. Ernst, E. Trizac, and A. Barrat, J. Stat. Phys. **124**, 549 (2006).
 - [15] K. Vollmayr-Lee, T. Aspelmeier, and A. Zippelius Phys. Rev. E **83**, 011301 (2011).
 - [16] M. I. García de Soria, P. Maynar, and E. Trizac, Phys. Rev. E **85**, 051301 (2012).
 - [17] M. I. García de Soria, P. Maynar, and E. Trizac, Phys. Rev. E **87**, 022201 (2013).
 - [18] A slight variant of the model can be found in [48, 60, 61].
 - [19] C. Josserand, A. V. Tkachenko, D. M. Mueth, and H. M. Jaeger, Phys. Rev. Lett. **85**, 3632 (2000).
 - [20] J. J. Brey and A. Prados, Phys. Rev. E **63**, 061301 (2001).
 - [21] A. Barrat and V. Loreto, Europhys. Lett. **53**, 297 (2001).
 - [22] J. J. Brey and A. Prados, J. Phys: Cond. Matt. **14**, 1489 (2002).
 - [23] P. Richard, M. Nicodemi, R. Delannay, P. Ribière, and D. Bideau, Nature Materials **4**, 121 (2005).
 - [24] Ph. Ribière, P. Richard, P. Philippe, D. Bideau, and R. Delannay, Eur. Phys. J. E **22**, 249 (2007).
 - [25] A. J. Kovacs, Adv. Polym. Sci. (Fortschr. Hochpolym. Forsch.) **3**, 394 (1963).
 - [26] A. J. Kovacs, J. J. Aklonis, J. M. Hutchinson, and A. R. Ramos, J. Pol. Sci. **17**, 1097 (1979).
 - [27] S. A. Brawer, Phys. Chem. Glasses **19**, 48 (1978).
 - [28] L. Berthier and J. P. Bouchaud, Phys. Rev. B **66**, 054404 (2002).
 - [29] S. Mossa S and F. Sciortino, Phys. Rev. Lett. **92**, 045504 (2004).
 - [30] G. Aquino, A. Allahverdyan, and T. M. Nieuwenhuizen, Phys. Rev. Lett. **101**, 015901 (2008).
 - [31] A. Prados and J. J. Brey, J. Stat. Mech. P02009 (2010).
 - [32] E. Bouchbinder and J. S. Langer, Soft Matter **6**, 3065 (2010).
 - [33] G. Diezemann and A. Heuer, Phys. Rev. E **83**, 031505 (2011).
 - [34] M. Ruiz-García and A. Prados, Phys. Rev. E **89**, 012140 (2014).
 - [35] J. Lutsko, Phys. Rev. E **63**, 061211 (2001).
 - [36] J. J. Brey, M. J. Ruiz-Montero, and F. Moreno, Phys. Rev. E **69**, 051303 (2004).
 - [37] A. Prados and E. Trizac, Phys. Rev. Lett. **112**, 198001 (2014), arXiv:1404.6162.

- [38] N. V. Brilliantov and T. Pöschel, *Europhys. Lett.* **74**, 424 (2006).
- [39] L. Landau and E. Lifshitz, *Physical Kinetics* (Pergamon Press, New York, 1981).
- [40] E. Trizac, *Physical Review Letters* **88**, 160601 (2002).
- [41] J. Piasecki, E. Trizac, M. Droz *Physical Review E* **66**, 066111 (2002).
- [42] There is a typo in the expression for B of Ref. [16], concretely in the sign of the term in the denominator proportional to $(62 - 30\alpha)$, which has been corrected upon writing Eq. (17).
- [43] It can be noted that under the stochastic forcing with drag studied in Ref. [48], the excess kurtosis does also change sign at $\alpha = 1/\sqrt{2}$, keeping a functional dependence on α that is close to that considered here.
- [44] G. Bird, *Molecular Dynamics and the Direct Simulation of Gas Flows* (Clarendon, Oxford, 1994).
- [45] A long enough t_w is easily attained by starting from a high enough initial value of the driving ξ_0 , that is, a high enough granular temperature.
- [46] For $\alpha = 0.8$, the theoretical estimates of the excess kurtosis are $a_2^{\text{HCS}} = -0.02243$ and $a_2^s = -0.01349$, so that $a_2^{\text{HCS}} - a_2^s = -0.00895$, while the simulation values are $a_2^{\text{HCS}} = -0.02635$ and $a_2^s = -0.01495$, which lead to $a_2^{\text{HCS}} - a_2^s = -0.01140$.
- [47] Note however that for the moment $n = 1$ (related to the collision frequency), the inequality is reversed. The change of sign of the correction, between $n = 1$ and $n = 3$, illustrates the subtleness of the effect. Platykurtic shapes exhibit depleted distributions for small velocities, then enhanced population around the thermal scale, and again depletion for slightly larger velocities (not speaking about the truly large velocity tail, which does not matter here, and which is overpopulated [7, 62]). It is the balance of these over/under populations that leads to Eq. (36) above. Note also that Eq. (36) explains the presence of the contribution $3a_2/16$ in Eq. (7), see also [7].
- [48] M. G. Chamorro, F. Vega-Reyes, and V. Garzó, *J. Stat. Mech. (Theor. Exp.)* P07013 (2013).
- [49] Let us remember that, in molecular systems, the role of the granular temperature is usually played by the volume or the energy, while the role of the driving is played by the bath temperature. The steady value of the granular temperature is an increasing function of the driving, a trend that is similar to the increase of the equilibrium value of the energy or volume with increasing bath temperature.
- [50] N. G. van Kampen, *Stochastic Processes in Physics and Chemistry* (North-Holland, Amsterdam, 1997).
- [51] A. Puglisi, A. Baldassarri, and V. Loreto, *Phys. Rev. E* **66**, 061305 (2002).
- [52] A. Puglisi, A. Baldassarri, and A. Vulpiani, *J. Stat. Mech: Theor. Exp.* P08016 (2007).
- [53] A. Prados, A. Lasanta, and P. I. Hurtado, *Phys. Rev. Lett.* **107**, 140601 (2011); *Phys. Rev. E* **86**, 031134 (2012).
- [54] J. J. Brey, P. Maynar, and M. I. García de Soria, *Phys. Rev. E* **86**, 061308 (2012).
- [55] A. Sarracino, D. Villamaina, G. Gradenigo, A. Puglisi, *EPL* **92**, 34001 (2010).
- [56] A. Baldassarri, U. Marini Bettolo Marconi, and A. Puglisi, *Phys. Rev. E* **65**, 051301 (2002); *Europhys. Lett.* **58**, 14 (2002).
- [57] This has been very recently checked, see for instance Eq. (37) of Ref. [63], in which this kind of memory effect has been analyzed for a different thermostat, within the first Sonine approximation.
- [58] The case of the so-called Gaussian thermostat would then be special, because it can be mapped onto the homogeneous cooling state. Thus, all the time dependence of the system is encoded in the temperature and, in particular, the value of the excess kurtosis is known [11].
- [59] P. Résibois and M. de Leener, *Classical Kinetic Theory of Fluids* (John Wiley, New York, 1977).
- [60] A. Puglisi, V. Loreto, U. M. B. Marconi, and A. Vulpiani, *Phys. Rev. E* **59**, 5582 (1999).
- [61] V. V. Prasad, S. Sabhapandit and A. Dhar, *EPL* **104**, 54003 (2013).
- [62] A. Barrat and E. Trizac, *Eur. Phys. J. E* **11**, 99 (2003).
- [63] J. J. Brey, M. I. García de Soria, P. Maynar, and V. Buzón, arXiv:1404.6381.